

HD-THEP-94-38

SU(3) Flux Tubes in a Model of the stochastic Vacuum

Michael Rueter*

*Institut für theoretische Physik
Universität Heidelberg
Philosophenweg 16, D-69120 Heidelberg, FRG*

H.G. Dosch

*Institut für theoretische Physik
Universität Heidelberg
Philosophenweg 16, D-69120 Heidelberg, FRG*

Abstract

We calculate the squared gluon field strengths of a heavy $q\bar{q}$ -pair in the model of the stochastic vacuum. We observe that with increasing separation a chromo-electric flux tube is built. The properties of the emerging flux tube are investigated.

*e-mail: rueter@next3.thphys.uni-heidelberg.de

1 Introduction

As is well known, the behavior of QCD at large distances is most probably not controlled by perturbation theory, but genuine non-perturbative effects are supposed to play an essential role in that infrared domain. This is indicated as well by analytical considerations [1] as by numerical calculations from lattice-QCD [2]. It is of course the ultimate desire to obtain analytical results directly from the QCD-Lagrangian, but successes in that direction are limited. At the moment all analytical results are based on models.

In the model of the stochastic vacuum (MSV) it is assumed that the complicated measure which emerges from the QCD-action in the region of slowly fluctuating fields can be described by a well behaved stochastic process [3] [4] [5]. This process can be visualized as a fluctuating background field representing the "physical vacuum".

In the most general form of the MSV one assumes that the above mentioned background field has a convergent cluster expansion, but for many specific applications phenomenologically useful results can only be obtained after further assumptions are made. One of these assumptions is that the stochastic vacuum can be described by a Gaussian process, i.e. only the 2-cumulant does not vanish. In a non-Abelian theory even the assumption of a Gaussian process has to be specified further, since the choice of the stochastic variables is ambiguous.

Our paper is organized as follows:

In section 2 we shortly present the model of the stochastic vacuum in a restricted form as it has been applied very successfully to soft hadron-hadron high-energy scattering [6] [7].

In section 3 we apply this restricted form of the model in order to calculate the squares of the field strengths of Euclidean Wegner-Wilson-loops. Especially we shall test the importance of some more technical assumptions described in section 2 and check the consistency of the approximations by investigating the Michael sum rule of the total energy stored in the field of the Wegner-Wilson-loop.

In section 4 we shall present the results, discuss them and compare, where possible, with lattice gauge calculations.

Throughout the paper we work in an **Euclidean** space-time continuum.

2 The model of the stochastic vacuum

A rather extensive description of the MSV as applied in this paper has been given in a recent publication [7], so we quote here for convenience only the main points.

The crucial ingredient of the MSV is the correlator between the gluon field strengths $F_{\mu\nu}^A(x, w)$ parallel transported to a reference point w

$$\mathbf{F}_{\mu\nu}(x, w) = \Phi^{-1}(x, w) \mathbf{F}_{\mu\nu}(x) \Phi(x, w), \quad (1)$$

where $\mathbf{F}_{\mu\nu}(x)$ is the Lie-algebra valued gluon field strength tensor and $\Phi(x, w)$ the path ordered non-Abelian Schwinger string:

$$\begin{aligned}\Phi(x, w) &= \mathcal{P} \exp \left[-ig \int_0^1 d\sigma (x - w)_\mu \mathbf{A}_\mu(w + \sigma(x - w)) \right] \\ \mathbf{F}_{\mu\nu}(x) &= \sum_{C=1}^{N_c^2 - 1} F_{\mu\nu}^C(x) \mathbf{t}^C\end{aligned}\quad (2)$$

N_c is the number of colors and unless otherwise stated we use the fundamental representation.

We make the crucial approximation that the correlator $\langle F_{\mu\nu}^A(x, w) F_{\rho\sigma}^B(y, w) \rangle_A$, i.e. the vacuum expectation value with respect to the non-perturbative background field, is independent of the reference point w . Then the most general form of the correlator is:

$$\begin{aligned}\langle g^2 F_{\mu\nu}^A(x, w) F_{\rho\sigma}^B(y, w) \rangle &= \frac{\delta^{AB}}{N_c^2 - 1} \frac{\langle g^2 FF \rangle}{12} \left\{ (\delta_{\mu\rho} \delta_{\nu\sigma} - \delta_{\mu\sigma} \delta_{\nu\rho}) \kappa D(z^2/a^2) \right. \\ &\quad \left. + \frac{1}{2} \left(\frac{\partial}{\partial z_\nu} (z_\sigma \delta_{\mu\rho} - z_\rho \delta_{\mu\sigma}) + \frac{\partial}{\partial z_\mu} (z_\rho \delta_{\nu\sigma} - z_\sigma \delta_{\nu\rho}) \right) (1 - \kappa) D_1(z^2/a^2) \right\} \quad (3)\end{aligned}$$

where $z = x - y$.

The fundamental parameters of the model are the correlation length a and the gluon condensate $\langle g^2 FF \rangle = \langle g^2 F_{\mu\nu}^C F_{\mu\nu}^C \rangle$.

The factors in eq.(3) are chosen in such a way that $D(0) = D_1(0) = 1$.

By evaluating the expectation value of a Wegner-Wilson-loop with the correlator (3) and Gaussian factorization one obtains the potential for a static q- \bar{q} -pair [8]

$$\begin{aligned}V(r) &= \frac{\langle g^2 FF \rangle a^3}{48N_C} \left\{ 2r \int_0^r d\rho \int_{-\infty}^{\infty} d\tau \kappa D(\rho^2 + \tau^2) \right. \\ &\quad \left. + \int_0^r \rho d\rho \int_{-\infty}^{\infty} d\tau (-2\kappa D(\rho^2 + \tau^2) + (1 - \kappa) D_1(\rho^2 + \tau^2)) \right\}.\end{aligned}\quad (4)$$

In an Abelian gauge theory without monopoles, where the homogeneous Maxwell equation must hold, only the second structure in eq.(3) can occur, i.e. we must have $\kappa = 0$. However, in a non-Abelian theory there is no reason for κ to be zero and it is the tensor structure proportional to κ which leads to the linear rising potential (first term in equation 4) and hence confinement.

From comparison with hadron spectroscopy, high-energy scattering [7] and lattice gauge calculations [9] the input to the right hand side of eq.(3) is pretty well fixed:

$$D(z^2/a^2) = -6A_4 \int \frac{d^4 k}{(2\pi)^4} \frac{k^2}{(k^2 + 1)^4} \exp \left(i \frac{k(z/a)}{\lambda_4} \right)$$

$$\begin{aligned}
&= \frac{|z/a|}{\lambda_4} \left[K_1 \left(\frac{|z/a|}{\lambda_4} \right) - \frac{1}{4} \frac{|z/a|}{\lambda_4} K_0 \left(\frac{|z/a|}{\lambda_4} \right) \right] \\
D_1(z^2/a^2) &= -4A_4 \int \frac{d^4k}{(2\pi)^4} \frac{1}{(k^2 + 1)^3} \exp \left(i \frac{k(z/a)}{\lambda_4} \right) \\
&= \frac{|z/a|}{\lambda_4} K_1 \left(\frac{|z/a|}{\lambda_4} \right)
\end{aligned} \tag{5}$$

with $\lambda_4 = \frac{8}{3\pi}$, $A_4 = -8\pi^2$, $a = 0.35\text{fm}$, $\langle g^2 FF \rangle = 2.39\text{GeV}^4$ and $\kappa = 0.74$. The K_μ are the modified Bessel-functions.

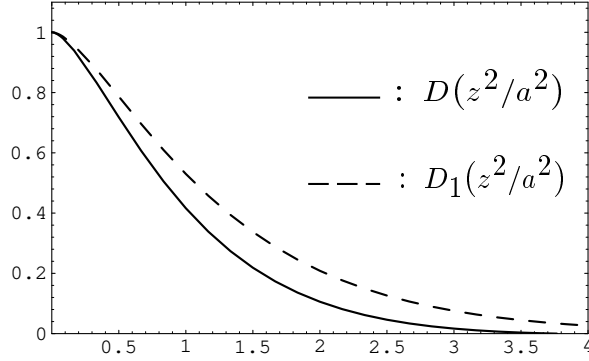


Figure 1: The functions $D(z^2/a^2)$ and $D_1(z^2/a^2)$ of eq.(5)

3 The squared components of the gluon field tensor

In this section we evaluate the tensor of the squared field strengths in the presence of a Wegner-Wilson-loop.

We introduce as usual the Wegner-Wilson-loop over a contour \mathcal{C}

$$\langle W[\mathcal{C}] \rangle = \text{tr } \mathcal{P} \langle \exp \left\{ -ig \oint_{\mathcal{C}} \mathbf{A}_\mu(x) dx_\mu \right\} \rangle \tag{6}$$

The plaquette $P_{\alpha\beta}(x)$ is a Wegner-Wilson-loop over a square in α, β -direction centered at x with side length R_P .

One easily obtains

$$P_{\alpha\beta}(x) = N_c - \frac{1}{4} R_P^4 g^2 \sum_C F_{\alpha\beta}^C(x) F_{\alpha\beta}^C(x) + \mathcal{O}(R_P^8) \tag{7}$$

where there is **no summation** over α and β on the r.h.s.

The non-perturbative vacuum expectation value of $P_{\alpha\beta}$ is related to the gluon conden-

sate:

$$\sum_{\alpha < \beta} \langle P_{\alpha\beta} \rangle = 6N_c - \frac{1}{8} R_P^4 \langle g^2 FF \rangle + \mathcal{O}(R_P^8) \quad (8)$$

To calculate the square of the gluon field strengths in the presence of a static quark-antiquark-pair we define the quantity [10] [11]

$$\Delta F_{\alpha\beta}^2(x) \equiv \frac{4}{R_P^4} \frac{\langle W[\mathcal{C}] P_{\alpha\beta}(x) \rangle - \langle W[\mathcal{C}] \rangle \langle P_{\alpha\beta}(x) \rangle}{\langle W[\mathcal{C}] \rangle}. \quad (9)$$

Here \mathcal{C} is the Wegner-Wilson-loop corresponding to a static $q\bar{q}$ -pair with side length R_W in 3-direction and T in 4-direction centered at the origin (see figure 2).

In the limit $R_P \rightarrow 0$ the elements of the tensor (9) are the differences between the expectation values of the squared elements of the gluon field strength tensor in the presence of the $q\bar{q}$ -pair and the fluctuations of the non-perturbative vacuum.

In order to evaluate $\Delta F_{\alpha\beta}^2(x)$ in the model of the stochastic vacuum we first transform as usual the path ordered line-integrals in the Wegner-Wilson-loops into surface ordered surface-integrals with the help of the non-Abelian Stokes-theorem [12].

$$\begin{aligned} \langle W[\mathcal{C}] \rangle &= \text{tr } \mathcal{P} \langle \exp \left\{ -ig \oint_{\mathcal{C}} \mathbf{A}_\mu(x) dx_\mu \right\} \rangle \\ &= \text{tr } \mathcal{P}_{\mathcal{S}} \langle \exp \left\{ -ig \int_{\mathcal{S}} \mathbf{F}_{\mu\nu}(x, w) d\sigma_{\mu\nu} \right\} \rangle \end{aligned} \quad (10)$$

The surface \mathcal{S} is bordered by the loop \mathcal{C} and contains the reference point w . The indices of the surface elements are restricted to $\mu < \nu$ throughout this paper.

Expanding the exponentials in eq.(9) we obtain:

$$\begin{aligned} \Delta F_{\alpha\beta}^2(x) &= \frac{4}{R_P^4} \frac{1}{\langle W \rangle} \left(\sum_{n=1}^{\infty} (-i)^n \int \cdots \int^{\text{surfaceordered}} d\sigma_{\mu_1\nu_1}^W \cdots d\sigma_{\mu_n\nu_n}^W \text{tr} [\mathbf{t}^{a_1} \cdots \mathbf{t}^{a_n}] \times \right. \\ &\quad \int \int d\sigma_{\mu\nu}^P d\sigma_{\rho\sigma}^P \times \frac{(-i)^2}{2!} \text{tr} [\mathbf{t}^a \mathbf{t}^b] \langle g^n F_{\mu_1\nu_1}^{a_1} \cdots F_{\mu_n\nu_n}^{a_n} g^2 F_{\mu\nu}^a F_{\rho\sigma}^b \rangle - \\ &\quad \sum_{n=1}^{\infty} (-i)^n \int \cdots \int^{\text{surfaceordered}} d\sigma_{\mu_1\nu_1}^W \cdots d\sigma_{\mu_n\nu_n}^W \text{tr} [\mathbf{t}^{a_1} \cdots \mathbf{t}^{a_n}] \int \int d\sigma_{\mu\nu}^P d\sigma_{\rho\sigma}^P \times \\ &\quad \left. \frac{(-i)^2}{2!} \text{tr} [\mathbf{t}^a \mathbf{t}^b] \langle g^n F_{\mu_1\nu_1}^{a_1} \cdots F_{\mu_n\nu_n}^{a_n} \rangle \langle g^2 F_{\mu\nu}^a F_{\rho\sigma}^b \rangle \right) \end{aligned} \quad (11)$$

Here we have neglected the higher terms in the expansion of $P_{\alpha\beta}$ since they are in higher order of R_P . In eq.(11) we have two loops and hence two surfaces each containing the

same point w . We have thus chosen the surfaces as sliding sides of a pyramid based either on the Wegner-Wilson-loop ($d\sigma^W$) or on the plaquette ($d\sigma^P$) (see figure 2).

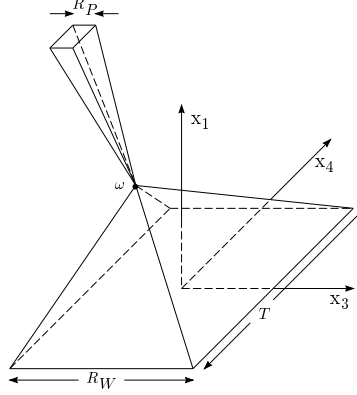


Figure 2: The two pyramids touching each other at the reference point w

We use the factorization of the color components of the field strength tensor as in [13] and [14], i.e. for example

$$\begin{aligned} \langle F^{C_1}(1)F^{C_2}(2)F^{C_3}(3)F^{C_4}(4) \rangle &= \langle F^{C_1}(1)F^{C_2}(2) \rangle \langle F^{C_3}(3)F^{C_4}(4) \rangle + \\ &\quad \langle F^{C_1}(1)F^{C_3}(3) \rangle \langle F^{C_2}(2)F^{C_4}(4) \rangle + \\ &\quad \langle F^{C_1}(1)F^{C_4}(4) \rangle \langle F^{C_2}(2)F^{C_3}(3) \rangle, \end{aligned} \quad (12)$$

where $F^{C_i}(i) \equiv F_{\mu_i \nu_i}^{C_i}(x_i, w)$

and analogously for all other expectation values. We obtain

$$\begin{aligned} \Delta F_{\alpha\beta}^2(x) &= \frac{4}{R_P^4} \frac{1}{\langle W \rangle} \left(\sum_{n=1}^{\infty} (-i)^{2n} \int \cdots \int \text{surfaceordered} d\sigma_{\mu_1 \nu_1}^W \cdots d\sigma_{\mu_{2n} \nu_{2n}}^W \text{tr} [\mathbf{t}^{a_1} \cdots \mathbf{t}^{a_{2n}}] \times \right. \\ &\quad \int \int d\sigma_{\mu\nu}^P d\sigma_{\rho\sigma}^P \frac{(-i)^2}{2!2!} \left[\sum_{\text{pairs}}^{\alpha_1, \beta_1 \cdots \alpha_n, \beta_n} \langle g^2 F_{\mu_{\alpha_1} \nu_{\alpha_1}}^{a_{\alpha_1}} F_{\mu_{\beta_1} \nu_{\beta_1}}^{a_{\beta_1}} \rangle \cdots \right. \\ &\quad \left. \left. \langle g^2 F_{\mu_{\alpha_{n-1}} \nu_{\alpha_{n-1}}}^{a_{\alpha_{n-1}}} F_{\mu_{\beta_{n-1}} \nu_{\beta_{n-1}}}^{a_{\beta_{n-1}}} \rangle \times \langle g^2 F_{\mu_{\alpha_n} \nu_{\alpha_n}}^{a_{\alpha_n}} F_{\mu\nu}^a \rangle \langle g^2 F_{\mu_{\beta_n} \nu_{\beta_n}}^{a_{\beta_n}} F_{\rho\sigma}^a \rangle \right] \right). \quad (13) \end{aligned}$$

Of the $2n$ field strengths running over the pyramid of the loop \mathcal{C} two are correlated with a $F_{\mu\nu}^C$ on the pyramid of the plaquette and the other $(2n-2)$ among one another. As soon as the two field strengths of one of the latter $(n-1)$ -pairs are not direct neighbors in surface ordering, this ordering is suppressed by at least a factor a/L as compared to the fully ordered ones (a is the correlation length and L the linear extension of the loop \mathcal{C}). We now neglect **in any order of the expansion** of the exponentials all terms

which are not fully ordered, i.e. which are suppressed by at least a factor a/L . For all fully ordered expressions the traces in eq.(13) are identical and one obtains:

$$\begin{aligned} \Delta F_{\alpha\beta}^2(x) &= \frac{4}{R_P^4} \frac{1}{\langle W \rangle} \left(\sum_{n=1}^{\infty} \frac{(-i)^{2n+2} \cdot N_c}{4(2N_c)^n (N_c^2 - 1)} \int \cdots \int^{\text{surfaceordered}} d\sigma_{\mu_1\nu_1}^W \cdots d\sigma_{\mu_{2n}\nu_{2n}}^W \times \right. \\ &\quad \left. \int \int d\sigma_{\mu\nu}^P d\sigma_{\rho\sigma}^P \left[\sum_{\text{pairs}}^{\alpha_1, \beta_1 \cdots \alpha_n, \beta_n} \langle g^2 F_{\mu_{\alpha_1}\nu_{\alpha_1}}^{C_1} F_{\mu_{\beta_1}\nu_{\beta_1}}^{C_1} \rangle \cdots \right. \right. \\ &\quad \left. \left. \langle g^2 F_{\mu_{\alpha_{n-1}}\nu_{\alpha_{n-1}}}^{C_{n-1}} F_{\mu_{\beta_{n-1}}\nu_{\beta_{n-1}}}^{C_{n-1}} \rangle \times \langle g^2 F_{\mu_{\alpha_n}\nu_{\alpha_n}}^{C_n} F_{\mu\nu}^{C_n} \rangle \langle g^2 F_{\mu_{\beta_n}\nu_{\beta_n}}^{C_{n+1}} F_{\rho\sigma}^{C_{n+1}} \rangle \right] \right) \end{aligned} \quad (14)$$

where the N_c -factors are due to the traces.

Now the integrand is symmetric and we may replace the ordered surface integrations by unconstrained ones, correcting for the larger phase space by the factor $1/(2n)!$:

$$\begin{aligned} \Delta F_{\alpha\beta}^2(x) &= \frac{4}{R_P^4} \frac{1}{\langle W \rangle} \left(\sum_{n=1}^{\infty} \frac{(-i)^{2n+2} \cdot N_c}{4(2N_c)^n (N_c^2 - 1) (2n)!} \int \cdots \int d\sigma_{\mu_1\nu_1}^W \cdots d\sigma_{\mu_{2n}\nu_{2n}}^W \times \right. \\ &\quad \left. \int \int d\sigma_{\mu\nu}^P d\sigma_{\rho\sigma}^P \left[\sum_{\text{pairs}}^{\alpha_1, \beta_1 \cdots \alpha_n, \beta_n} \langle g^2 F_{\mu_{\alpha_1}\nu_{\alpha_1}}^{C_1} F_{\mu_{\beta_1}\nu_{\beta_1}}^{C_1} \rangle \cdots \right. \right. \\ &\quad \left. \left. \langle g^2 F_{\mu_{\alpha_{n-1}}\nu_{\alpha_{n-1}}}^{C_{n-1}} F_{\mu_{\beta_{n-1}}\nu_{\beta_{n-1}}}^{C_{n-1}} \rangle \times \langle g^2 F_{\mu_{\alpha_n}\nu_{\alpha_n}}^{C_n} F_{\mu\nu}^{C_n} \rangle \langle g^2 F_{\mu_{\beta_n}\nu_{\beta_n}}^{C_{n+1}} F_{\rho\sigma}^{C_{n+1}} \rangle \right] \right) \end{aligned} \quad (15)$$

Performing the integration over each correlator separately we obtain:

$$\begin{aligned} \Delta F_{\alpha\beta}^2(x) &= \frac{4}{R_P^4} \frac{1}{\langle W \rangle} \left(\sum_{n=1}^{\infty} \frac{(-i)^{2n+2} \cdot N_c}{4(2N_c)^n (N_c^2 - 1) 2^{n-1} (n-1)!} \times \right. \\ &\quad \left(\int \int d\sigma_{\mu\nu}^P d\sigma_{\rho\sigma}^W \langle g^2 F_{\mu\nu}^C F_{\rho\sigma}^C \rangle \right)^2 \times \left(\int \int d\sigma_{\mu\nu}^W d\sigma_{\rho\sigma}^W \langle g^2 F_{\mu\nu}^C F_{\rho\sigma}^C \rangle \right)^{n-1} \left. \right) \\ &= \frac{4(-i)^4}{8 \cdot R_P^4 (N_c^2 - 1)} \frac{1}{\langle W \rangle} \left(\int \int d\sigma_{\mu\nu}^P d\sigma_{\rho\sigma}^W \langle g^2 F_{\mu\nu}^C F_{\rho\sigma}^C \rangle \right)^2 \times \\ &\quad \left(\sum_{n=0}^{\infty} \frac{(-i)^{2n}}{2^n n! (2N_c)^n} \left(\int \int^{\text{frei}} d\sigma_{\mu_1\nu_1}^W d\sigma_{\mu_2\nu_2}^W \langle g^2 F_{\mu\nu}^C F_{\rho\sigma}^C \rangle \right)^n \right) \end{aligned} \quad (16)$$

In the approximation used the sum is just $\frac{\langle W \rangle}{N_c}$ and the final result is

$$\Delta F_{\alpha\beta}^2(x) = \frac{4}{R_P^4} \frac{(-i)^4}{8N_C(N_C^2 - 1)} \left[\int \int d\sigma_{\mu\nu}^W d\sigma_{\rho\sigma}^P \langle g^2 F_{\mu\nu}^C F_{\rho\sigma}^C \rangle \right]^2. \quad (17)$$

We note that in the integral one surface element is connected to the Wegner-Wilson-loop (indicated by the index W) and one to the plaquette oriented in α, β -direction (indicated by P).

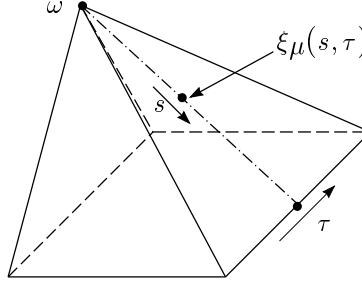


Figure 3: Parametrization of the sliding sides of a pyramid. s and $\tau \in [0, 1]$.

We now parametrize the surfaces as indicated in figure 3 and obtain with eq.(3):

$$\begin{aligned}
 \Delta F_{\alpha\beta}^2(x) = & \frac{4}{R_P^4} \frac{1}{(N_C^2 - 1)8N_C} \left[\sum_{\text{surfaces}} \int_0^1 ds_W ds_P d\tau_W d\tau_P \frac{< g^2 FF >}{12} \right. \\
 & \sum_{\substack{\mu < \nu \\ \rho < \sigma}} \frac{\partial (\xi_\mu^W(s_W, \tau_W), \xi_\nu^W(s_W, \tau_W))}{\partial (s_W, \tau_W)} \cdot \frac{\partial (\xi_\rho^P(s_P, \tau_P), \xi_\sigma^P(s_P, \tau_P))}{\partial (s_P, \tau_P)} \times \\
 & \left. \left\{ (\delta_{\mu\rho} \delta_{\nu\sigma} - \delta_{\mu\sigma} \delta_{\nu\rho}) \kappa D(z^2/a^2) + \right. \right. \\
 & \left. \left. \frac{1}{2} \left(\frac{\partial}{\partial z_\nu} (z_\sigma \delta_{\mu\rho} - z_\rho \delta_{\mu\sigma}) + \frac{\partial}{\partial z_\mu} (z_\rho \delta_{\nu\sigma} - z_\sigma \delta_{\nu\rho}) \right) (1 - \kappa) D_1(z^2/a^2) \right\} \right]^2 \quad (18)
 \end{aligned}$$

Here $z = \xi^W - \xi^P$ and the sum goes over the 16 different surface combinations parametrized by $\xi_\mu^W(s_W, \tau_W)$ and $\xi_\mu^P(s_P, \tau_P)$.

Since we are interested in the limit $R_P \rightarrow 0$ the integration over τ_P becomes trivial if we expand the expression around $\tau_P = 1/2$. We found that in all cases the limit $R_P \rightarrow 0$ was practically reached for $R_P \leq \frac{1}{6}a$.

Numerically the limit of static quarks was reached for $T \geq 6a$. But in order to study the static case we took the limit $T \rightarrow \infty$ analytically.

4 Results and Discussion

4.1 General results

The reference point w plays a crucial role in the non-Abelian Stokes-theorem and it has to be common to both surfaces in order to apply the MSV. Its choice influences

the results. Even for the application of the MSV to calculate a simple Wegner-Wilson-loop the resulting area law refers to the area including the reference point [15]. This is certainly one of the less pleasant features of the model and a consequence of the approximation of the complicated measure of the QCD-action by a Gaussian one. If we deform the surface, necessarily higher cumulants must be occur, since the result has to be independent of the surface. For the one loop case the MSV is in accordance with phenomenology and lattice calculations, if the minimal surface is chosen. We therefore have always chosen the minimal surface in the evaluation of a Wegner-Wilson-loop by the MSV in the Gaussian form.

To calculate $\Delta F_{\alpha\beta}^2(x)$ we proceed the same way. We choose the reference point in such a way, that the total resulting surface of the sliding sides of the pyramids is minimal. Since the surface of the plaquette is considered in the limit $R_P \rightarrow 0$, this means, that the reference point w has to be in the plane of the loop \mathcal{C} . This will always be our standard choice. In order to investigate the influence of the position, we will later also study the case where the reference point has an arbitrary position on the connection line between the plaquette \mathcal{P} and the loop.

We first concentrate on the typical non-Abelian tensor structure determined by the correlation function D .

It can be seen by symmetry arguments that for that case the difference of the square of the magnetic field strengths, i.e. the plaquette $P_{\alpha\beta}(x)$ with no time (x_4) component, vanishes identically. This means that the magnetic background field is not affected by the static color charges.

The electric field perpendicular to the Wegner-Wilson-loop is also practically not affected but only the difference of the squared electric field parallel to the loop.

In both cases the squared electric field difference is negative, i.e. the presence of the static source diminishes the vacuum fluctuations.

In figure 8 we display the value of the squared field strength parallel to the spatial loop extension $\Delta F_{34}^2(x) = - \langle g^2 E_z^2(x_3, r) \rangle_{q\bar{q}-\text{vacuum}}$ as a function of the coordinates $r = \sqrt{x_1^2 + x_2^2}$ and x_3 (the results are rotational invariant around the x_3 -axes) for different spatial separations R_W (see figure 2 for the choice of coordinates).

The squared field strength reaches its saturation value $\Delta F_{34}^2(x) \approx 14 \frac{\text{GeV}}{\text{fm}^3}$ for a spatial extension of the Wegner-Wilson-loop $R_W \approx 4a = 1.4\text{fm}$. The transversal extension of the flux tube, defined by

$$r_{\text{MS}} \equiv \sqrt{\frac{\int dr r r^2 \Delta F_{34}^2(0, r)}{\int dr r \Delta F_{34}^2(0, r)}}, \quad (19)$$

is practically independent of R_W and about 1.8 times the correlation length a (see figure 9).

As mentioned above, the quantity $\Delta F_{34}^2(x)$ is the difference between the squared field strength in the presence of a static $q\bar{q}$ -pair and the non-perturbative vacuum field strength. In figure 10 we display the unsubtracted squared field tensor of the color source in units of the vacuum gluon condensate $\langle g^2 FF \rangle$.

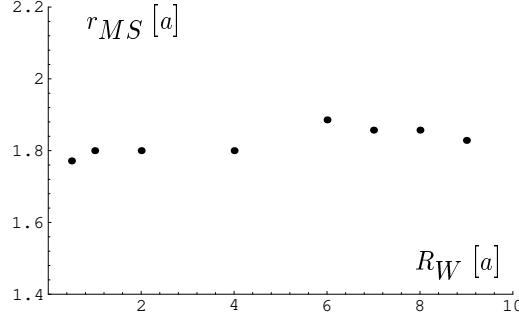


Figure 9: The transversal extension r_{MS} of the squared electric field as a function of the quark separation R_W .

As can be seen, the presence of the static source has only a moderate influence on the global vacuum-structure ($\approx 10\%$).

Now we discuss the second correlation function D_1 . The contribution of this correlator to $\Delta F_{\alpha\beta}^2(x)$ is numerically much less important than that of the correlator D . For small distances this is mostly due to the factor $(1 - \kappa) = 0.26$, but for large distances the fact that with this correlator no string is formed becomes decisive.

Again the square of the magnetic field is not influenced by the static source, but now the squared parallel **and** perpendicular electric fields are of the same size and build up a spherical distribution. In figure 13 we show $\Delta F_{14}^2(x_3, r) + \Delta F_{24}^2(x_3, r) + \Delta F_{34}^2(x_3, r)$ for the correlator D_1 .

4.2 Michael sum rule

The total field energy due to the presence of the static quark source is just the potential energy of the quarks. We thus have a relation between the expectation value of the Wegner-Wilson-loop and the spatial integral over the sum of $\Delta F_{\alpha\beta}^2(x)$. This is one of the Michael sum rules [16]. In our case we can not test this sum rule absolutely, since we do not know g^2 . We can however estimate the effective value of g^2 from potential models of quarkonia to $g^2 \approx 6$ [17]. The Michael sum rule yields than a very sensitive test for the some more technical approximations made to calculate $\Delta F_{\alpha\beta}^2(x)$. We remind especially of the special choice of factorization and the neglect of all terms suppressed by at least a factor a/L in the expansion of the Wegner-Wilson-loop.

In figure 14 we display the numerically integrated energy density $\frac{1}{2g^2}(\Delta F_{14}^2 + \Delta F_{24}^2 + \Delta F_{34}^2)$ with $g^2 = 7.2$ and compare it to the $q\bar{q}$ -potential (4) as determined from the model of the stochastic vacuum.

We observe an almost perfect agreement between the two determinations even for distances which are small as compared to the correlation length a . (The error of the points is about the same size as the points due to the numerical integration.) The agreement in form and the very reasonable value of $\alpha_s \approx 0.57$ for the effective strong interaction coupling show, that the approximations of the MSV are well consistent.

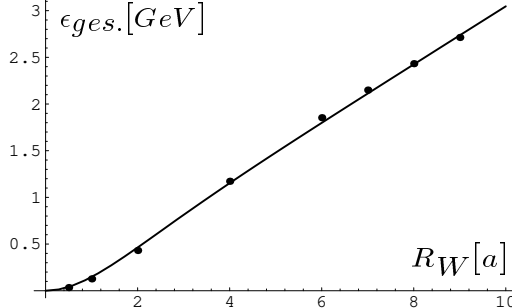


Figure 14: The total energy stored in the field (dots) compared with the potential of a $q\bar{q}$ -pair as obtained by eq.(4)

4.3 Color-Coulomb contribution

Having determined the effective α_s we are in the position to obtain an approximation to the full QCD-expression by adding to the non-perturbative results the color-Coulomb contribution. The result for the full energy density is displayed in figure 17 for $R_W = 2a$ and $R_W = 9a$.

For $R_W = 0.7\text{fm}$ the perturbative contribution increases the energy density in the middle of the flux tube from $0.65\frac{\text{GeV}}{\text{fm}^3}$ to $4.2\frac{\text{GeV}}{\text{fm}^3}$ and even for $R_W = 1.4\text{fm}$ this increase goes from $1.1\frac{\text{GeV}}{\text{fm}^3}$ to $1.9\frac{\text{GeV}}{\text{fm}^3}$. Since lattice calculations are typically working with Wegner-Wilson-loops of spatial expansion $R_W \approx 1\text{fm}$ the measured field strength is to a large extent a perturbative one. The magnitude of our full energy densities (SU(3)) agrees qualitatively with the scaled lattice results for SU(2) [18] [19] [20].

4.4 Dependence of the results on the reference point

In a non-Abelian gauge theory it is essential to transport the color content of the field strength correlator to a fixed reference point in order to obtain gauge covariant results. Such a reference point also occurs quite naturally in the non-Abelian Stokes-theorem as starting point of the surface ordering [15]. The final result for the expectation value of a Wegner-Wilson-loop must be independent of the choice of the reference point, but the result of the MSV calculation does depend on it, if the reference point is moved outside the surface under consideration. As discussed before the minimal surface is most adequate for the simplification of the measure of the QCD-action to a Gaussian one. Thus this has been our standard choice. Now we want to test the dependence of the results on the reference point, varying its position on the connection line between the plaquette and the loop as indicated in figure 18. $\alpha=0$ corresponds to our standard choice of $w!$ on the loop and for $\alpha=1$ the reference point is inside the plaquette.

In figure 19 we display the squared electric field parallel to the quark axis in the transversal plane between the two quarks ($\Delta F_{34}^2(0, r)$). In figure 20 we show the same

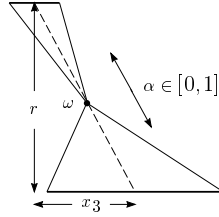


Figure 18: Definition of the parameter α which describes the position of the reference point w . $\alpha=0$ corresponds to our standard choice and for $\alpha=1$ the reference point is inside the plaquette.

field as a function of the position between the quarks with a distance of one correlation length from the $q\bar{q}$ -axis ($\Delta F_{34}^2(x_3, 1a)$). For the parameter α we took the values $\alpha = 0, \frac{1}{4}, \frac{1}{2}, \frac{3}{4}, 1$.

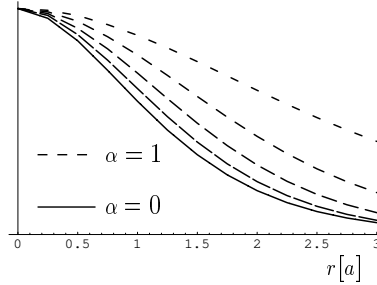


Figure 19: The squared electric field parallel to the $q\bar{q}$ -axis in the transversal plane between the two quarks ($\Delta F_{34}^2(0, r)$) for a quark separation $R_W = 6a$ and for different positions of the reference point w (see figure 18). The solid line is for $\alpha = 0$ and the values $\alpha = \frac{1}{4}, \frac{1}{2}, \frac{3}{4}, 1$ are plotted by subsequent shorter dashes.

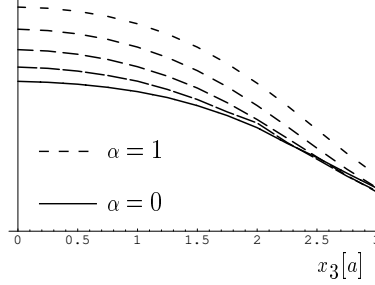


Figure 20: The squared electric field parallel to the $q\bar{q}$ -axis as a function of the position between the quarks with a distance of one correlation length from the $q\bar{q}$ -axis ($\Delta F_{34}^2(x_3, 1a)$) for a quark separation $R_W = 6a$ and for different positions of the reference point w (see figure 18).

As can be seen, the results are rather stable for $\alpha \leq \frac{1}{2}$ and the variation of α has only a limited numerical effect.

4.5 Summary

The MSV in its simplest form makes definite predictions on the non-perturbative contributions of the chromodynamic fields of a static $q\bar{q}$ -pair. The first result is that the expectation values of the squared magnetic and perpendicular electric field are not affected by the quark pair whereas the squared electric field parallel to the quark axis is diminished. This is in qualitative agreement with lattice gauge calculations of the connected linear field strengths [21]. The vacuum structure is quite stable, because the fluctuations of $\langle g^2 FF \rangle$ are decreased by only 10%.

With increasing quark separation a flux tube with constant width ($r_{\text{MS}} \approx 0.64\text{fm}$) and energy density of about $1 \frac{\text{GeV}}{\text{fm}^3}$ is built.

The approximations in the MSV made here respect the Michael sum rule with an effective strong coupling $\alpha_S = 0.57$. By adding the perturbative contribution with this coupling to the non-perturbative one we obtained the total energy density in agreement with lattice SU(2) gauge calculations [18] [19] [20].

Acknowledgements

We would like to thank O. Nachtmann for fruitful discussions.

References

[1] see e.g. A.H.Mueller, "The QCD Perturbation Series" in **QCD, 20 Years later**, P.M.Zerwas and H.A.Kastrup, World Scientific Singapore (1993)

- [2] see e.g. E.Laerman, "Interquark Forces" in **QCD, 20 Years later**, P.M.Zerwas and H.A.Kastrup, World Scientific Singapore (1993)
- [3] H.G.Dosch, *Phys.Lett.***B190** (1987) 177
- [4] H.G.Dosch, *Prog.Part.Nucl.Phys.***33** (1994) 121
- [5] H.G.Dosch, Y.A.Simonov, *Phys.Lett.***B205** (1988) 339
- [6] H.G.Dosch, E.Ferreira, A.Krämer, *Phys.Lett.***B289** (1992) 153
- [7] H.G.Dosch, E.Ferreira, A.Krämer, *Phys.Rev.***D50** (1994) 1992
- [8] Y.A.Simonov, *Nucl.Phys.***B324** (1989) 67
- [9] A.D.Giacomo, H.Panagopoulos, *Phys.Lett.***B285** (1992) 133
- [10] M.Fukugita, T.Niuya, *Phys.Lett.***B132** (1983) 374
- [11] J.W.Flower, S.W.Otto, *Phys.Lett.***B160** (1985) 128
- [12] N.E.Bralic, *Phys.Rev.***D22** (1980) 3090
- [13] H.G.Dosch, A.Krämer, *Phys.Lett.***B252** (1990) 669
- [14] H.G.Dosch, A.Krämer, *Phys.Lett.***B272** (1991) 114
- [15] Y.A.Simonov, *Sov.J.Nucl.Phys.***50** (1989) 134
- [16] C.Michael, *Nucl.Phys.***B280** (1987) 13
- [17] E.Eichten, K.Gottfried, T.Kinoshita, K.D.Lane, T.M.Yan, *Phys.Rev.***D21** (1980) 203
- [18] R.W.Haymaker, Y.Peng, *Phys.Rev.***D47** (1993) 5104
- [19] R.W.Haymaker, J.Wosiek, *Phys.Rev.***D43** (1991) 2676
- [20] Browne, R.W.Haymaker, V.Singh, J.Wosiek, Preprint LSUHE-130-1992
- [21] L.Del Debbio, A.Di Giacomo, Yu.A.Simonov, *Phys.Lett.***B332** (1994) 111

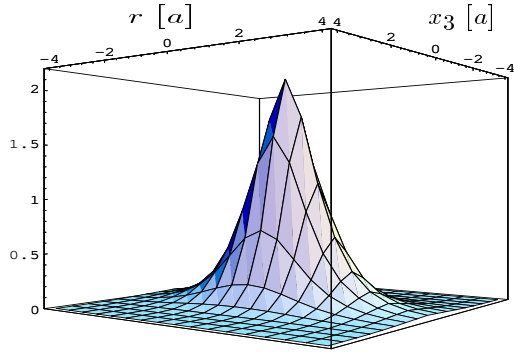


Figure 4: $R_W = 1a$, $a = 0.35\text{fm}$

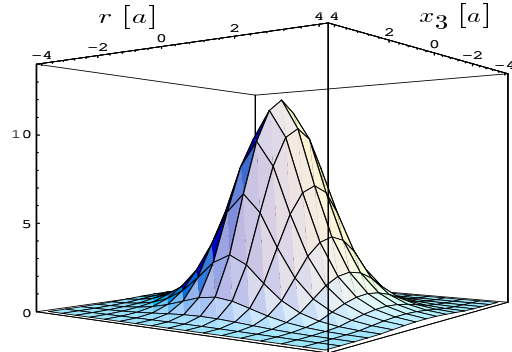


Figure 5: $R_W = 4a$, $a = 0.35\text{fm}$

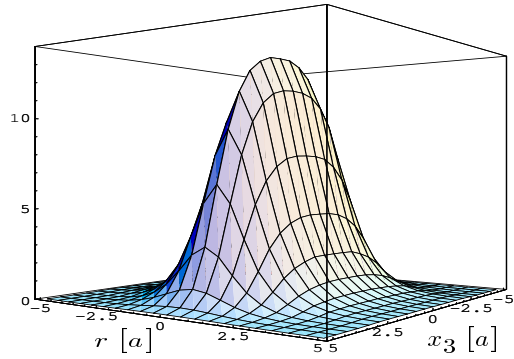


Figure 6: $R_W = 7a$, $a = 0.35\text{fm}$

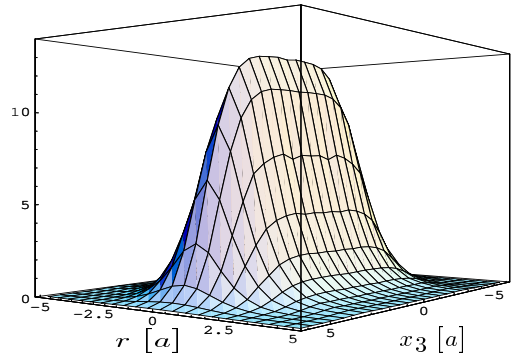


Figure 7: $R_W = 9a$, $a = 0.35\text{fm}$

Figure 8: Difference of the squared electric field parallel to the quark (x_3) axis ($- \langle g^2 E_z^2(x_3, r) \rangle_{q\bar{q}-\text{vac}}$) in $\frac{\text{GeV}}{\text{fm}^3}$ for different quark separations R_W .

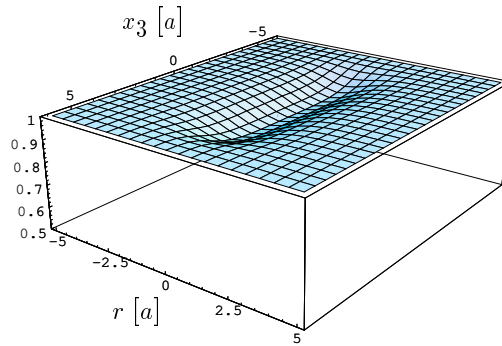


Figure 10: The unsubtracted squared field tensor $\langle g^2 FF \rangle_{q\bar{q}}$ in units of $\langle g^2 FF \rangle_{\text{vacuum}}$ for a quark separation $R_W = 9a$.

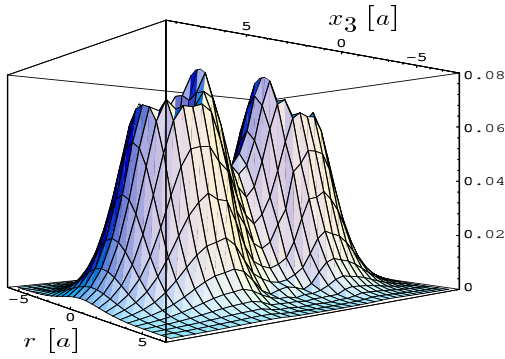


Figure 11: $R_W = 7a$, $a = 0.35\text{fm}$

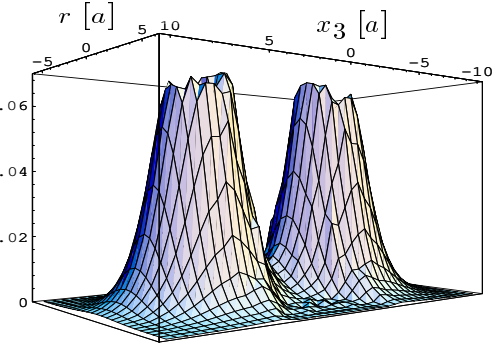


Figure 12: $R_W = 9a$, $a = 0.35\text{fm}$

Figure 13: Difference of the squared electric field ($- \langle g^2 E^2(x_3, r) \rangle_{q\bar{q}-\text{vac}}$) in $\frac{\text{GeV}}{\text{fm}^3}$ caused by the correlator D_1 for two different quark separations R_W .

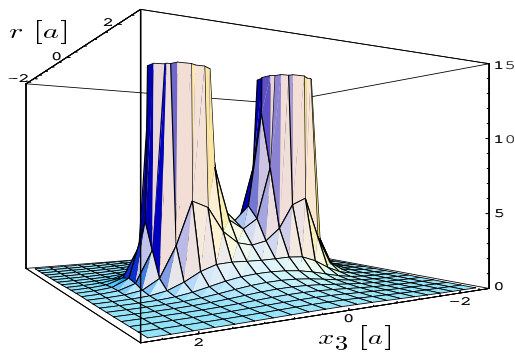


Figure 15: $R_W = 2a$, $a = 0.35\text{fm}$

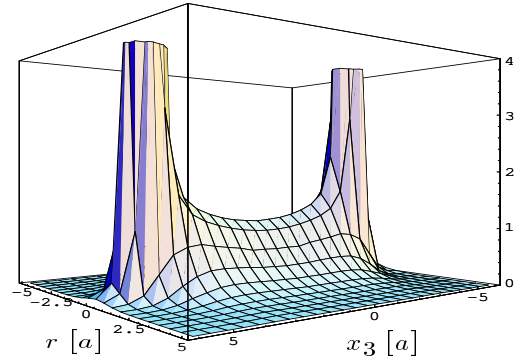


Figure 16: $R_W = 9a$, $a = 0.35\text{fm}$

Figure 17: The full energy density of a $q\bar{q}$ -pair caused by the non-perturbative correlator and the color-Coulomb contribution with $\alpha_S = 0.57$ in $\frac{\text{GeV}}{\text{fm}^3}$ for two different quark separations.